Comparison of the Effects of Organoclay Loading on the Curing and Mechanical Properties of Organoclay-Filled Epoxidised Natural Rubber Nanocomposites and Organoclay-Filled Natural Rubber Nanocomposites

R. N. Hakim and H. Ismail*

Polymer Division, School of Materials and Mineral Resources Engineering, Universiti Sains Malaysia, 14300 Nibong Tebal, Pulau Pinang, Malaysia

*Corresponding author: hanafi@eng.usm.my

Abstract: *Comparison between epoxidised natural rubber (ENR) and natural rubber (NR) filled with organoclay in terms of curing characteristics, tensile properties, thermal stability and morphology were studied. Organoclay loadings from 2 to 10 phr loading were used in this study. The nanocomposites were compounded using laboratory-sized two roll mills and cured at 150°C. The results indicate that the tensile strength and tensile modulus reached a maximum at 8 phr of organoclay, but elongation at break and thermal stability increased with increasing organoclay loading. Overall results show that organoclay-filled ENR nanocomposites exhibited shorter processing time and higher tensile properties than organoclay-filled NR nanocomposites. The enhanced properties were due to the homogenous dispersion of individual silicate layers in the ENR matrix, which is shown in the X-ray diffraction (XRD), scanning electron microscopy (SEM) and transmission electron microscopy (TEM) results.*

Keywords: organoclay, epoxidised natural rubber, natural rubber, nanocomposites

Abstrak: *Perbandingan di antara getah asli terepoksida (ENR) dan getah asli (NR) terisi tanah liat organo dari segi ciri-ciri pematangan, sifat tensil, kestabilan terma dan morfologi telah dikaji. Pembebanan tanah liat organo daripada 2 hingga 10 bsg telah digunakan di dalam kajian ini. Komposit nano telah disebatikan menggunakan mesin penggulung kembar berskala makmal dan dimatangkan pada 150(insert darjah disini)C. Keputusan menunjukkan kekuatan tensil dan modulus tensil mencapai nilai maksimum pada 8 bsg tanah liat organo tetapi pemanjangan pada takat putus dan kestabilan terma meningkat dengan peningkatan pembebanan tanah liat organo. Keputusan keseluruhan menunjukkan komposit nano ENR terisi tanah liat organo mempunyai masa pemprosesan yang lebih pendek dan sifat tensil yang lebih tinggi daripada komposit nano NR. Peningkatan sifat-sifat ini adalah disebabkan oleh penyerakan individu lapisan silikat yang homogeny di dalam matrik ENR sebagaimana ditunjukkan di dalam keputusan pembelauan sinar-x (XRD), mikroskopi electron imbasan (SEM) dan mikroskopi electron transmisi (TEM).*

Kata kunci: tanah liat organo, getah asli terepoksida, getah asli, komposit nano

1. INTRODUCTION

The idea of nanocomposites, which is widely credited to the researchers at Toyota Central Research Laboratories (Japan), has became very popular in the past decade and has been reviewed in various references.[1,2] The newfound interest is mostly due to the high reinforcing effectiveness of nano-sized fillers when dispersed on the nanometer instead of the micrometer scale. However, to achieve nano-reinforcement, the layers of the nanofillers have to be completely separated from one another viz. delamination or exfoliation.

Various researchers[3–5] studied an array of polymer compounds to find the desired processing and vulcanisate properties, as well as high performance. Epoxidised natural rubber (ENR) is one interesting example. ENR rubber has properties that more closely resemble those of synthetic rubbers than natural rubber.[4,5] It can offer unique properties, such as good oil resistance and low gas permeability coupled with high strength when compounded with the appropriate compounding ingredients.

Ultimately, natural rubber (NR) (cis-1,4-polyisoprene) has the best mechanical strength properties, which makes it an important and irreplaceable material in dynamically loaded applications such as tyres and engine mounts.[6] Brydson[6] also wrote that, apart from dynamic mechanical strength, NR has also been noted to have outstanding tear resistance or cut resistance. The high strength of NR is certainly due to its ability to undergo strain-induced crystallisation.

NR also had shown excellent improvements in mechanical properties, thermal properties, barrier properties and flame-retardant properties when compounded with organoclays.[7–11] In this work, ENR 50 was selected due to its high polarity, which should be beneficial when compounding with polar fillers, such as organoclays. Organoclay was chosen because of its abundant availability and for the fact that its intercalation chemistry has been studied for a long time. The comparison between the organoclay-filled ENR nanocomposites and organoclay-filled NR nanocomposites was made because of the anticipation of marked improvements in properties of organoclay-filled ENR nanocomposites compared to organoclay-filled NR nanocomposites. The comparison was also made because there have been no studies on the comparison of organoclay-filled NR nanocomposites against ENR nanocomposites.

Therefore, the major aim of this work was to compare the curing characteristics and mechanical properties of organoclay-filled epoxidised natural rubber (ENR 50) nanocomposites and organoclay-filled natural rubber (SMR L) nanocomposites.

2. EXPERIMENTAL

2.1 Rubber Recipe

ENR with 50 mol% epoxidation (ENR 50) having a Mooney viscosity of ML (1+4)100°C = 140 was obtained from the Kumpulan Guthrie, Malaysia. SMR L was purchased from Rubber Research Institute Malaysia (RRIM). Commercial organoclay was purchased from Nanocor, Inc. USA (Nanomer 1.30T). Nanomer 1.30T is a surface-modified montmorillonite with 70%–85% clay and 15wt%–30 wt% octadecylamine. The mean dry particle size of the organoclay was 18–23 μm.

2.2 Sample Preparation

Rubber mixing was carried out in accordance with ASTM D3184 using a laboratory-sized (160 × 320 mm) two roll mill (Model XK-160) maintained at 70 ± 5°C. The various rubber additives were added to the masticated natural rubber prior to the addition of organoclay, and sulphur was added last. The organoclay rubber nanocomposites were conditioned at 23 ± 2°C for 24 h prior to cure assessment. The formulation of the compounds is described in Table 1.

Table 1: Formulation of organoclay filled NR and ENR nanocomposites.

Materials	Part per hundred rubber (phr)
SMR L / ENR 50	100
Sulphur	2.5
Zinc Oxide	5.0
Stearic Acid	3.0
CBS[a]	0.5
6PPD[b]	1.0
Organoclay	0, 2, 4, 6, 8, 10

[a] N-cyclohexyl-2-benzothiazyl sulphonamide (CBS)
[b] N-(1,3-dimethylbutyl)-N'-phenyl-p-phenylenediamine (6PPD)

2.3 Measurement of Cure Characteristics

The cure characteristics of the rubber compounds were studied using a Monsanto Moving Die Rheometer (MDR 2000) according to ISO 3417 at 150°C. The respective cure times as measured by t_{90}, scorch times t_2, maximum torque, minimum torque, etc., were determined from the rheograph. The compounds were then compression moulded at 150°C using the respective cure times, t_{90}.

2.4 Measurement of Rubber-Filler Interactions

Cured samples with dimensions of 30 × 5 × 2 mm were swollen in toluene in a dark environment until equilibrium swelling was achieved, which normally took 48 h at 25°C. The samples were dried in an oven at 60°C until they achieved constant weight. The Lorenz and Park equation has been applied to study the rubber-filler interaction.
According to this equation:

$$\frac{Q_f}{Q_g} = ae^{-z} + b \tag{1}$$

In this study, Q was determined (the weight of toluene uptake per gram of rubber hydrocarbon) according to the expression:

$$Q = \frac{Swollen\ weight\ -\ Dried\ weight}{Original\ weight}$$

The subscripts *f* and *g* in Eq. (1) refer to filled and gum vulcanisates, respectively. *Z* is the ratio by weight of filler to the rubber hydrocarbon in the vulcanisate, whilst a and b are constants. The higher the Q_f/Q_g values, the lower the extent of the interaction between the filler and the matrix.

2.5 Measurement of Tensile Properties

Dumb-bell shaped samples were cut from the moulded sheets, and tensile test were performed at a cross-head speed of 500 mm min^{-1} using Lloyds Universal Testing Machine according to ISO 37.

2.6 SEM Analysis for Tensile Fracture Surface

The fracture surfaces of the organoclay-filled NR nanocomposites and organoclay-filled ENR nanocomposites were investigated with a Leica Cambridge S-360 SEM. The fracture ends of specimen were mounted on aluminium stubs and sputter coated with a thin layer of gold to avoid electrostatic charging during examination.

2.7 Thermo Gravimetric Analysis (TGA)

Thermodegradation of the nanocomposites was determined using thermo gravimetric analysis (TGA) with Perkin Elmer Analyser. Thermograms of approximately 10 mg samples were recorded from 50°C to 600°C at a heating rate of 10°C min^{-1} under nitrogen flow.

2.8 XRD Analysis

An X-ray diffractometer (Cu-Ko radiation) was used to evaluate the dispersion state of the organoclay in the NR matrix using a Siemens D5000 model (40 kV generator voltages). The samples were scanned at a low angle (from 2° to 10°) at a scanning rate of 2° min^{-1}.

3. RESULTS AND DISCUSSION

3.1 Cure Characteristics

Figures 1 and 2 and Table 2 show the results for the scorch time, t_2, and cure time, t_{90}, for both organoclay-filled NR nanocomposites and organoclay-filled ENR nanocomposites, respectively. For both nanocomposites, it can be seen that the scorch time and cure time decreased with increasing amounts of organoclay filler. The trend observed was due to the presence of octadecylamine (modification agents) from the organoclay. It has been reported[11,12] that amine groups facilitate the curing reaction of NR compounds.

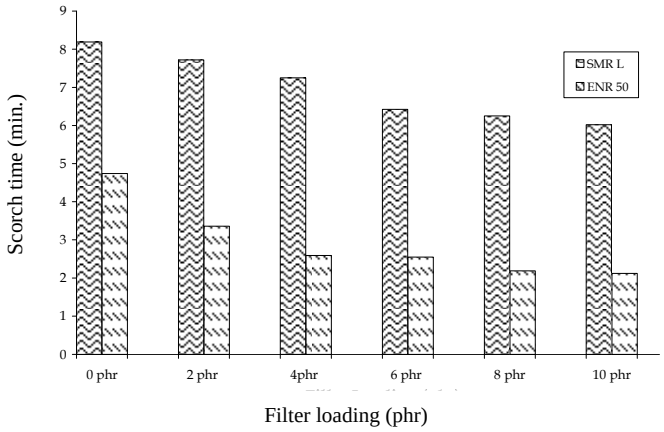

Figure 1: The effect of organoclay loading on scorch time of NR and ENR nanocomposites.

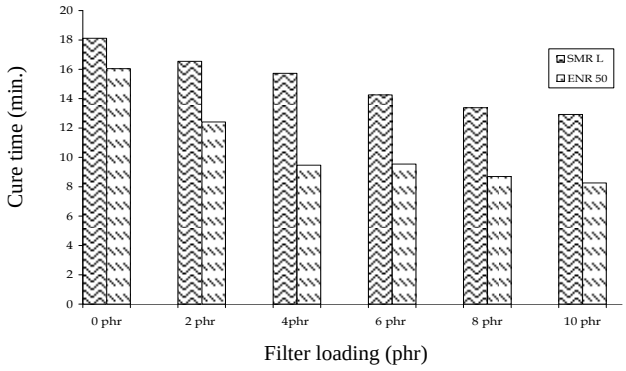

Figure 2: The effect of organoclay loading on cure time of NR and ENR nanocomposites.

Comparing ENR 50 against SMR L, the scorch time and cure time of the organoclay-filled ENR 50 were much lower than those of the organoclay-filled SMR L. According to Varghese et al.,[13] this is likely linked to a transition metal complexing in which the sulphur and amine-groups of the organoclay and of chain opening reaction of epoxy group in ENR 50 that participated in the vulcanisation reaction. This leads to a lowering of the scorch time and cure time of the organoclay-filled ENR compared to those of the NR nanocomposites.

Table 2: Scorch time (ts_2), cure time (t_{90}), maximum torque (M_H) and tensile strength for organoclay-filed NR and ENR nanocomposites.

Types of Nanocomposites	Scorch time (ts_2)	Cure time (t_{90})	Max torque (M_H)	Tensile strength (MPa)
0 phr Organoclay-Filled NR Nancocomposites	8.19	18.11	49.00	16.70
0 phr Organoclay-Filled ENR Nancocomposites	4.74	16.04	52.70	16.14
2 phr Organoclay-Filled NR Nancocomposites	7.72	16.55	49.90	22.69
2phr Organoclay-Filled ENR Nancocomposites	3.36	12.41	55.10	23.60
4phr Organoclay-Filled NR Nancocomposites	7.25	15.73	49.90	23.20
4phr Organoclay-Filled ENR Nancocomposites	2.59	9.47	56.70	24.52
6 phr Organoclay-Filled NR Nancocomposites	6.42	14.26	52.20	23.81
6phr Organoclay-Filled ENR Nancocomposites	2.55	9.54	57.50	25.20
8 phr Organoclay-Filled NR Nancocomposites	6.25	13.38	55.20	23.99
8phr Organoclay-Filled ENR Nancocomposites	2.19	8.69	61.70	25.81
10 phr Organoclay-Filled NR Nancocomposites	6.02	12.93	51.70	23.30
10phr Organoclay-Filled ENR Nancocomposites	2.12	8.26	57.00	23.45

Figure 3 shows the results of maximum torque, M_H, for both organoclay-filled NR nanocomposites and the organoclay-filled ENR compound. For both nanocomposites, it can be seen that with an increased amount of organoclay, the maximum torque, M_H, increased up to an optimum of 8 phr. Then, the maximum torque decreased at higher filler loading. The increase in the maximum torque suggests that some degree of reinforcement occurred in both nanocomposites.

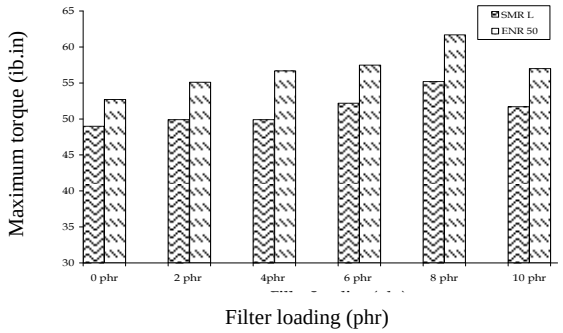

Figure 3: The effect of organoclay loading on maximum torque of NR and ENR nanocomposites.

Comparing the NR nanocomposites and ENR nanocomposites, the minimum torque and maximum torque of ENR nanocomposites showed higher values than those of the NR nanocomposites. According to Gelling,[14] the presence of isolated double bonds in ENR 50 will reduce the formation of intermolecular sulphide links. This will increase the efficiency of the vulcanisation process of ENR, which results in the higher values of the minimum and maximum torques.

3.2 Mechanical Properties

Figure 4 and Table 2 show the effect of organoclay loading on the tensile strength of organoclay-filled NR and ENR nanocomposites. For both nanocomposites, it can be seen that the optimum tensile strength was achieved around 8 phr of organoclay loading. This result indicates that the intercalation and exfoliation of NR or ENR into the clay silicate layer improved the interaction between organoclay and natural rubber, which increased the tensile strength. However, at 10 phr of organoclay loading, the tensile strength started to decrease slightly, which can be attributed to a reduction in interaction due to the agglomeration of the clay, as shown later in XRD and TEM analyses.

Comparing the NR and ENR nanocomposites, the tensile strengths of the organoclay-filled ENR nanocomposites were higher than those of the organoclay-filled NR nanocomposites. The alkyl ammonium chains of the organoclay contain polar groups, which leads to better compatibility between this organoclay and ENR.

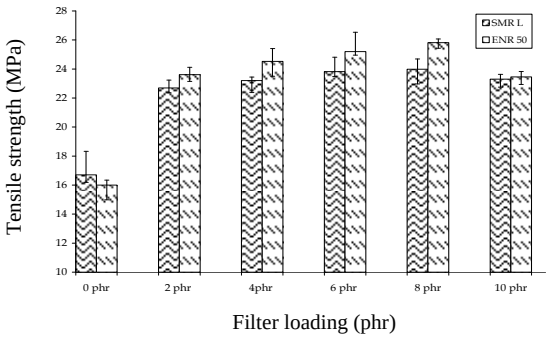

Figure 4: The effect of organoclay loading on tensile strength of NR and ENR nanocomposites.

Figures 5 and 6 show the effect of organoclay loading on stress at 100% elongation (M100) and stress at 300% elongation (M300) of NR and ENR nanocomposites. For both NR and ENR nanocomposites, M100 and M300 values increased with increasing organoclay loading until 8 phr of filler loading and then decreased with increasing loading of filler. This result indicates that the rubber-filler interactions are good until 8 phr and then became worse when the filler loadings were higher than 8 phr. This can be attributed to agglomeration of organoclay at high loading.

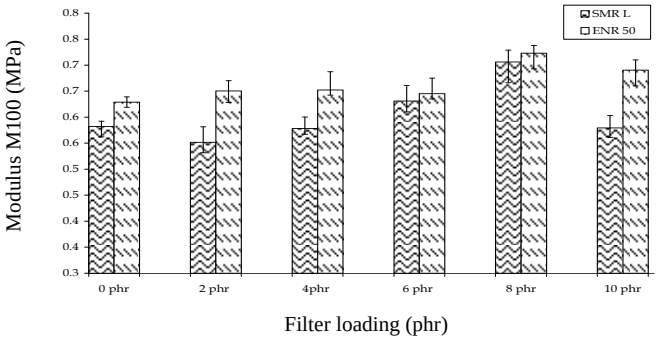

Figure 5: The effect of organoclay loading on tensile modulus M100 of NR and ENR nanocomposites.

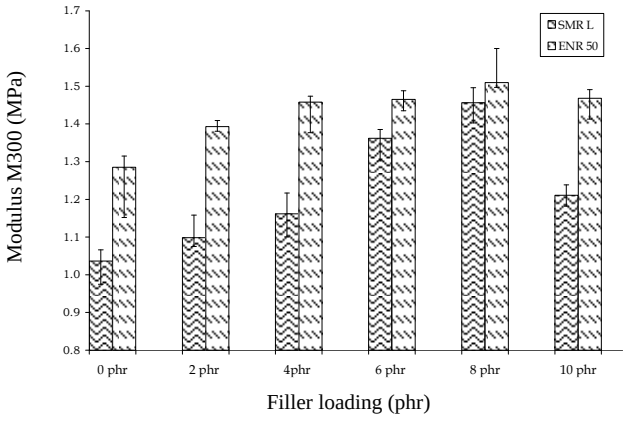

Figure 6: The effect of organoclay loading on tensile modulus M300 of NR and ENR nanocomposites.

Comparing organoclay-filled NR nanocomposites with organoclay-filled ENR nanocomposites, at a similar filler loading, both M100 and M300 for organoclay-filled NR nanocomposites were lower than those of ENR. The factor that contributed to this was the greater amount of chemical bonding between the ENR functional groups and the organoclay compared to NR with organoclay.

Figure 7 shows the effect of organoclay loading on elongation at break, E_b. For both SMR L and ENR 50, elongation at break increased with increasing filler loading. According to Ardhyanata et al.,[15] Ismail and Munusamy[16] and Varghese et al.,[13] this observation suggests that intercalation and exfoliation phenomena occurred, which resulted in high strength reinforcement at very low filler loading. The elongation of the rubbers was largely retained due to the low loading of organoclay.

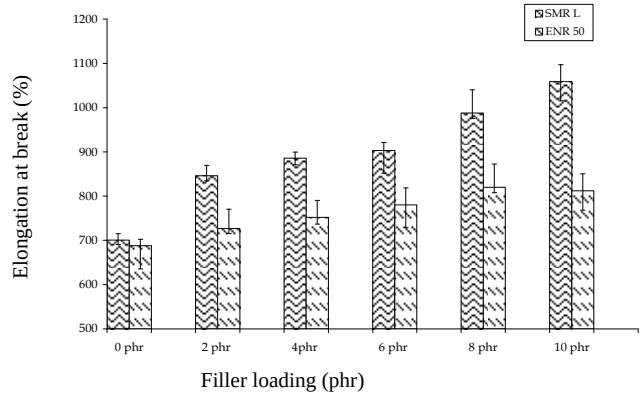

Figure 7: The effect of organoclay loading on elongation at breaking of NR and ENR nanocomposites.

At a similar filler content, organoclay-filled NR nanocomposites exhibited higher elongation at break, E_b than organoclay-filled ENR nanocomposites. Both rubbers exhibited relatively high values of elongation at break, but organoclay-filled NR had a higher elongation at break than ENR. This observation was mainly due to higher elasticity of SMR L compared to ENR 50.

3.3 Rubber-Filler Interaction

Figure 8 shows the effect of organoclay loading on the rubber-filler interaction, (Q_f/Q_g). For both SMR L and ENR 50, it can be seen that the rubber-filler interactions were good until 8 phr of filler loading and became poorer with further filler loading.

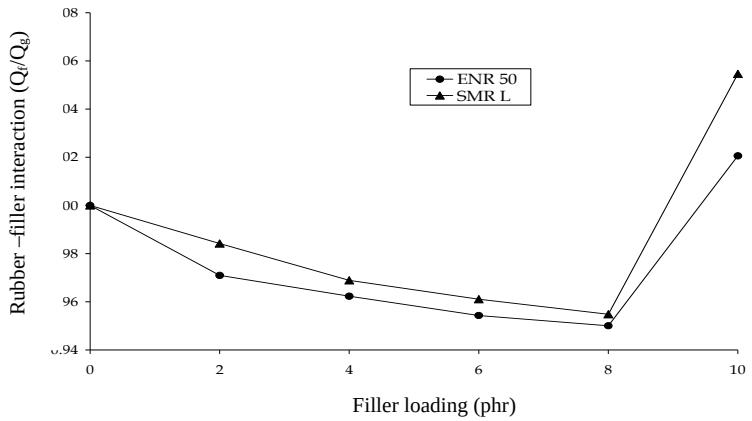

Figure 8: The effect of organoclay loading on rubber-filler interaction Q_f/Q_g of NR and ENR nanocomposites.

Comparing both NR and ENR nanocomposites, the ENR nanocomposites gave lower values of Q_f/Q_g, which confirmed that better interactions between organoclay and ENR occur. According to Arroyo et al.,[17] this can be attributed to the formation of chemical bonding between the ENR functional groups and the organoclay. ENR 50 is a polar rubber, whereas SMR L is a nonpolar rubber. It is generally observed that the mechanical response of mixing an organoclay closely related to its compatibility is a synergistic effect that is often obtained with miscible or partially compatible mixing. The partial compatibility was due to the epoxy groups of ENR 50 that interacted chemically with the hydroxyl groups of the filler surface and octadecylamine, a surface modifier of filler. This interaction occurred due to the higher polarity of ENR compared to NR, which resulted in more intercalation of rubber in between the intergalleries of the organoclay.

3.4 Scanning Electron Microscopy (SEM)

Figure 9 shows the tensile fracture surfaces of organoclay-filled ENR nanocomposites, while Figure 10 shows the tensile fracture surfaces of organoclay-filled NR nanocomposites at 0, 2, 8 and 10 phr of filler loading, respectively. Considering the results of the tensile strength in Figure 4 and the fracture surfaces in Figure 19, it seems that the rougher the fracture surface the better the tensile properties of the related nanocomposites are. A smooth fracture surface usually indicates low compatibility accompanied with premature, rather brittle-type fracture.[17]

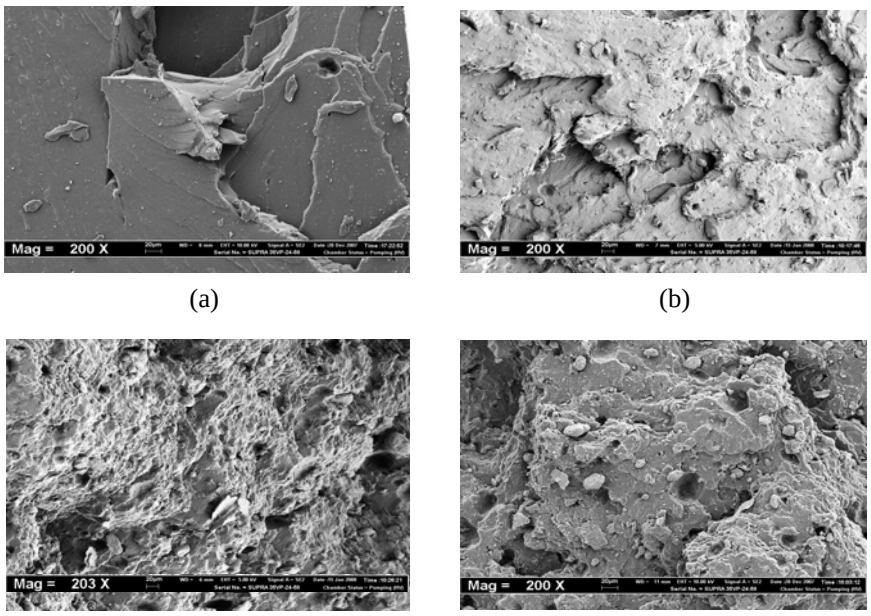

(a) (b)

(c) (d)

Figure 9: SEM micrographs showing tensile fracture surface of epoxidised NR nanocomposites: (a) 0 phr; (b) 2 phr; (c) 8 phr and (d) 10 phr.

At 0 phr, both NR and ENR nanocomposites exhibited a relatively smooth surface. At 2 phr, both NR and ENR exhibited rougher surfaces with many curved tearing with minimal voids or cavities. The appearance of a rough surface is due to the fact that failure starts on inhomogeneities located away from that of the major fracture plane. Final fracture occurs in that case via coalescence of the voided (cavitated) areas. It is still a matter of dispute whether the failure, i.e. voiding, starts within the intercalated clay particles or at their surfaces.[18] At 8 phr, both NR and ENR exhibited much rougher surfaces than at 2 phr, with minimal voids and cavities. There is a considerable visual evidence which shows that tensile strength increased as organoclay content increased up to 8 phr. At higher organoclay loading (10 phr), the tensile fracture surfaces exhibited more voids and cavities for both NR and ENR. Hence, increasing organoclay above 8 phr decreased the interaction between rubber-filler and led to poor filler dispersion. This observation validates the tensile results discussed earlier.

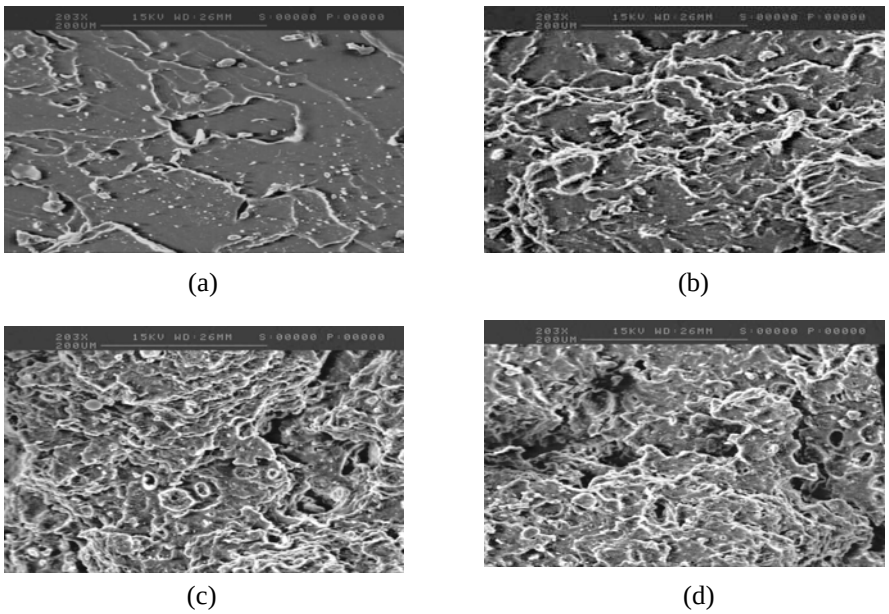

(a) (b)

(c) (d)

Figure 10: SEM micrographs showing tensile fracture surface of NR nanocomposites: (a) 0 phr (b) 2 phr (c) 8 phr (d) 10 phr.

Comparing the NR and ENR nanocomposite micrographs, the ENR nanocomposites exhibit relatively rougher tensile fracture surfaces, indicating higher strength than NR. It is expected that the hydroxyl groups of the filler surface are able to react with the epoxy groups of ENR, giving rise to a better interaction between the organoclay and ENR matrix.

3.5 Thermogravimetric Analysis (TGA)

Figure 11 shows the TG curves of ENR/organoclay nanocomposites filled with 2, 8 and 10 phr of organoclay loading, whereas Figure 12 shows the TG curves of NR/organoclay nanocomposites filled with 2, 8 and 10 phr of organoclay loading. Table 3 summarises the thermal degradation using the TGA curves in Figures 11 and 12. For ENR and NR gum vulcanisation, two steps of thermal degradation occured at 300°C–400°C. The second degradation corresponded to the degradation of the polyisoprene chain and is followed by volatilisation of the nanocomposite structure formed at higher temperature. Comparing ENR 50 and NR, the first degradation of ENR/organoclay nanocomposites occurred at higher temperatures compared to NR/organoclay nanocomposites. From Table 3, it is clear that the decomposition temperature at 5% weight loss ($T_{-5\%}$) and 50% weight loss ($T_{-50\%}$) for both ENR/organoclay and

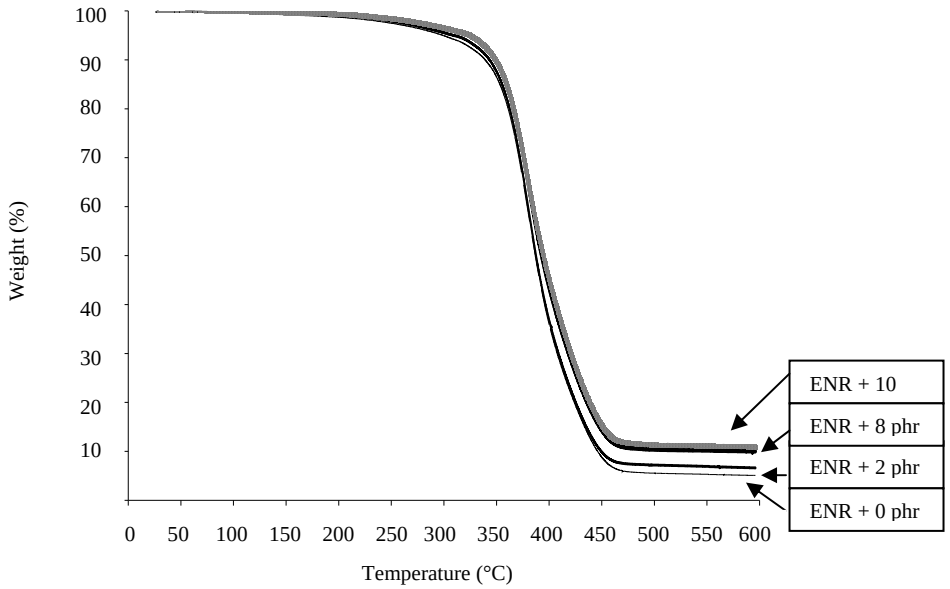

Figure 11: TG curves of ENR/organoclay nanocomposites filled with 2, 8 and 10 phr of organoclay loading surface of ENR nanocomposites.

NR/organoclay at 10 phr of organoclay loading happened at higher temperature than for 8 phr, 2 phr and 0 phr of organoclay. Moreover, the char residue of both nanocomposites also increased with increasing filler loading. The results indicate that incorporation of organoclay in both nanocomposites enhances thermal stability.

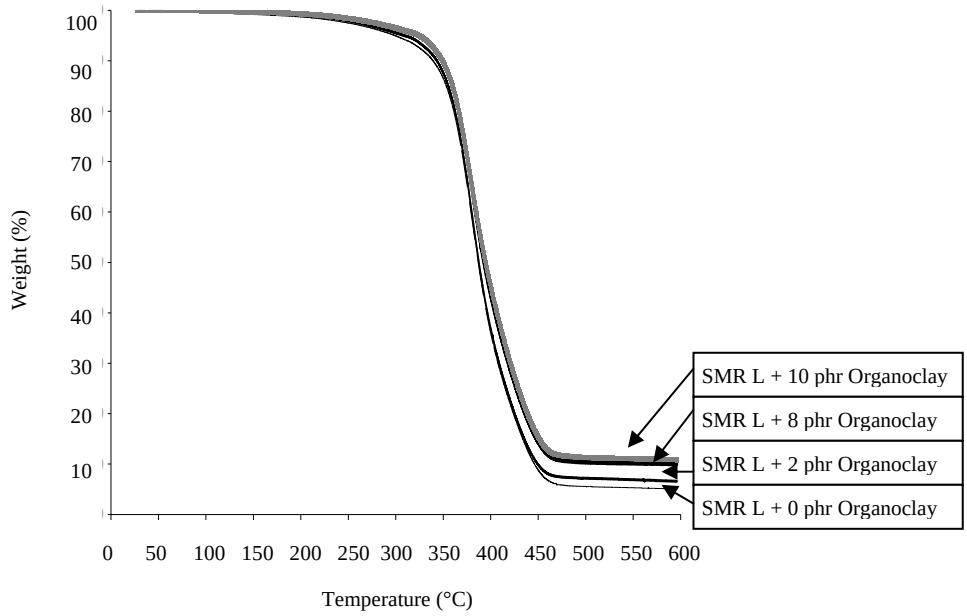

Figure 12: TG curves of NR/organoclay nanocomposites filled with 2, 8 and 10 phr of organoclay loading surface of NR nanocomposites.

Table 3: Thermal Properties of ENR/Organoclay versus NR/Organoclay Filled Natural Rubber Nanocomposites.

Organoclay loading	T_{-5}(°C)	T_{-50}(°C)	Residue Weight (%)
0 phr (ENR 50)	302.63	391.29	5.42
0 phr (SMR L)	298.99	386.77	5.08
2 phr (ENR 50)	309.86	389.63	6.93
2 phr (SMR L)	308.97	387.50	6.60
8 phr (ENR 50)	329.76	398.67	10.51
8 phr (SMR L)	323.41	392.50	10.00
10 phr (ENR 50)	329.88	398.64	11.03
10 phr (SMR L)	324.76	394.64	10.86

It is generally well accepted that the improved thermal stability for polymer-clay is mainly due to the formation of char, which hinders the out-diffusion of volatile decomposition products. This corresponds to the nanocomposites structure that formed at 10, 8 and 2 phr of organoclay loading, which improved the thermal stability of the material. The individual nanolayer is an effective shield to reduce the volatilisation of the degradation product. Gao et al.[20] reported that the thermal stability of a polymer was notably improved by incorporating small amounts of organoclay. The improvements of the thermal stabilities of a polymer by hybridising organoclay was due to the layered silicates of organoclay that make the path longer for the thermally decomposed volatiles to escape. The reason is that most of the thermally decomposed volatiles are captured by organoclay. Zanetti et al.[21] reported that in air, the nanocomposites present a significant delay of weight loss that may derive from the barrier effect due to the diffusion of both the volatile thermo-oxidation products to the gas phase and oxygen from the gas phase to the polymer. This barrier effect increases during volatilisation due to the reassembly of the layers on the surface of the polymer. Zhang et al.[22] reported that in nanocomposites, montmorillonite has excellent barrier properties, prevents the permeation of atmospherical air and assists the formation of char after thermal decomposition. At 10 phr of organoclay loading, the greater amount of remaining ashes (residue weight) were attributed to the high thermal stability of organoclay-filled NR nanocomposites.

Comparing ENR and NR, it is observed that the residual 5% weight loss ($T_{-5\%}$) and 50% weight loss ($T_{-50\%}$) of ENR and ENR/organoclay at 2, 8 and 10 phr all occurred at higher temperature than for NR and NR/organoclay. These results suggest that ENR/organoclay nanocomposites have higher thermal stability than NR/organoclay.

3.6 X-Ray Diffraction (XRD)

Figures 13 and 14 show the XRD spectra for the organoclay, ENR/organoclay and NR/organoclay nanocomposites with 2, 8 and 10 phr of organoclay, respectively. It can be seen that the organoclay showed a broad intense peak at around $2^{\circ} = 4.178$, corresponding to a basal spacing of 2.159 nm.

However, the X-ray diffraction patterns for both ENR and NR nanocomposites with 2, 8 and 10 phr of organoclay exhibited a disappearance of the diffraction peak at around $2° = 4.178$. This shows that during compounding, the penetration of ENR or NR chains in between the silicate layers occurred. However, this penetration did not completely result in disruption of the silicate stacks.

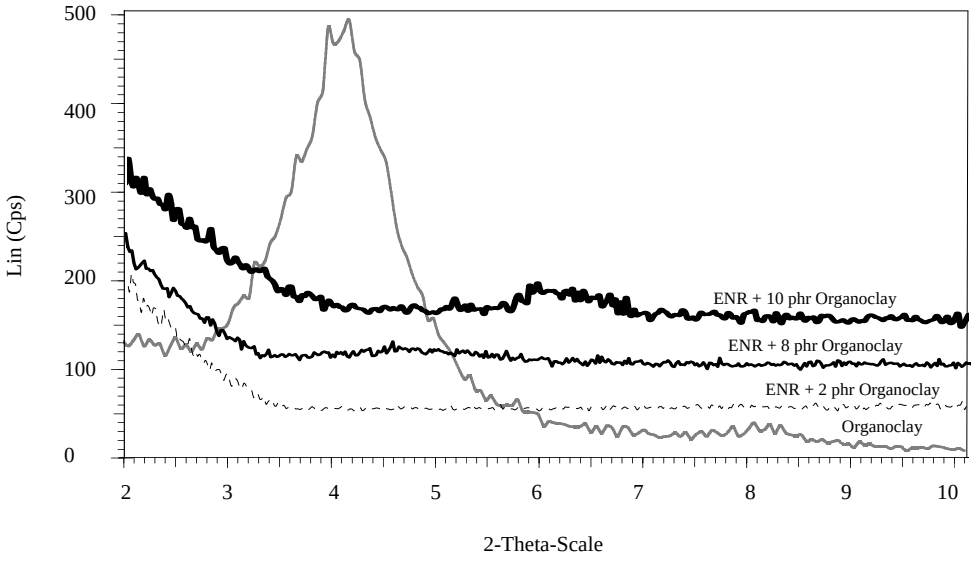

Figure 13: XRD patterns for organoclay-filled ENR nanocomposites.

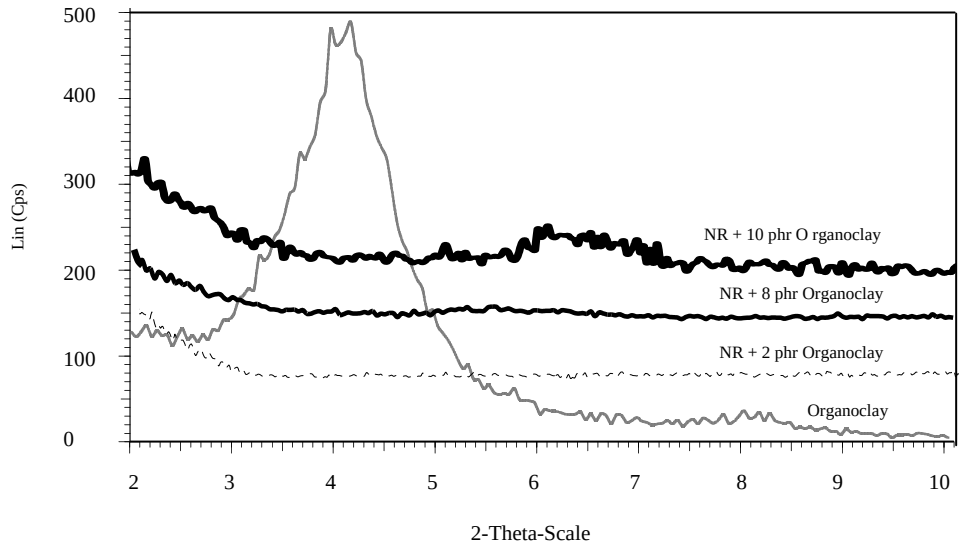

Figure 14: XRD patterns for organoclay-filled NR nanocomposites.

At 10 phr, a new peak developed for both ENR and NR at $2\theta = 6.158$ for ENR and $2\theta = 6.313$ for NR. This shows that at organoclay loadings higher than 8 phr, there were more agglomerates created particularly at 10 phr, thus reducing the tensile properties of both organoclay-filled ENR nanocomposites and organoclay-filled NR nanocomposites.

3.7 Transmission Electron Microscopy (TEM)

In order to further verify the existence of the organoclay dispersion in ENR 50 and SMR L, TEM observations were made. Figures 15, 16 and 17 show the TEM micrographs of organoclay-filled ENR nanocomposites at 2, 8 and 10 phr, respectively. Figures 18, 19 and 20 show the TEM micrographs of organoclay-filled NR nanocomposites at 2, 8 and 10 phr, respectively. These figures demonstrate that organoclay was well intercalated and exfoliated in the ENR 50 matrix, particularly at 8 phr of organoclay. According to Arroyo et al.,[17] due to the polarity of ENR, a better dispersion of organoclay in the ENR matrix has been observed. However, at 10 phr of organoclay, both of the nanocomposites exhibited some agglomeration of organoclays. All these observations are in concordance with the XRD patterns and confirmed a better dispersion of the organoclay in the case of ENR 50.

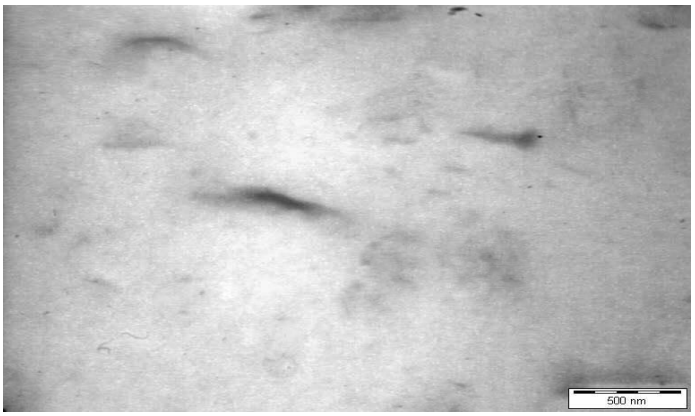

Figure 15: TEM micrograph for 2 phr organoclay-filled ENR nanocomposites.

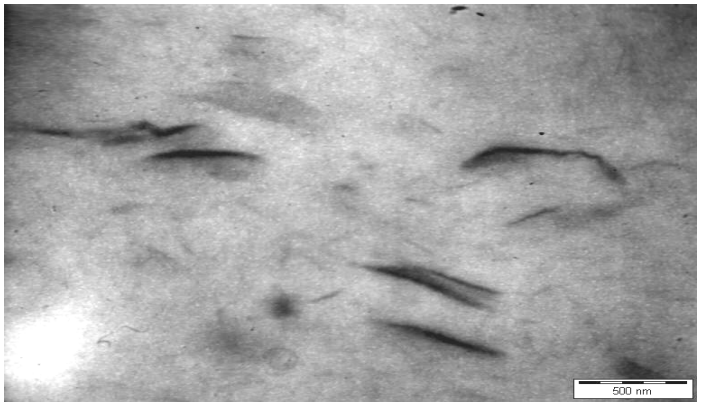

Figure 16: TEM micrograph for 8 phr organoclay-filled ENR nanocomposites.

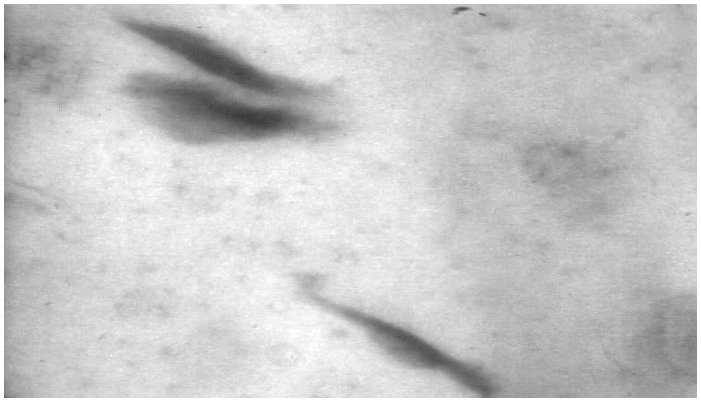

Figure 17: TEM micrograph for 10 phr organoclay-filled ENR nanocomposites.

Figure 18: TEM micrograph of NR/organoclay nanocomposites at 2 phr filler loading.

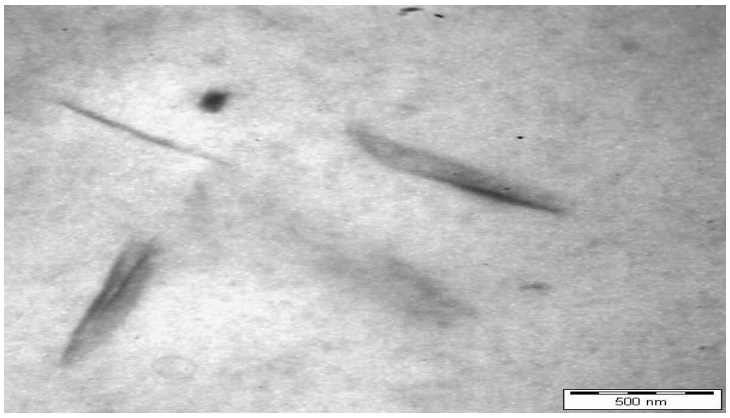

Figure 19: TEM micrograph of NR/organoclay nanocomposites at 8 phr filler loading.

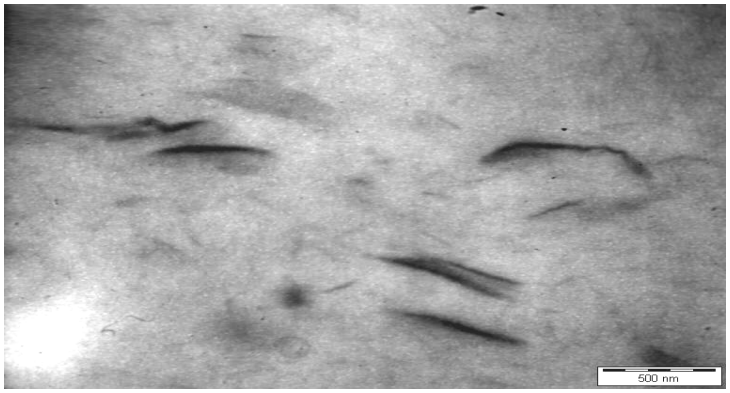

Figure 20: TEM micrograph of NR/organoclay nanocomposites at 10 phr filler loading.

4. CONCLUSION

The maximum torque increased with the addition of organoclay into NR nanocomposites. Moreover, the curing characteristics, i.e., the scorch time (t_2) and cure time (t_{90}), of the NR nanocomposites were shorter due to the presence of amine functional groups in the organoclay. The incorporation of organoclay into NR nanocomposites increased the tensile strength, elongation at break and rubber-filler interaction at optimum loading, i.e., 8 phr filler content. The enhanced properties were due to the homogeneous dispersion of individual silicate layers in the nanometer range in the NR matrix. XRD and TEM results indicated that the organoclay were intercalated and exfoliated at 8 phr of organoclay and partly exfoliated and re-aggregated at 10 phr of organoclay.

Tensile modulus, M100 and M300 and thermal stability improved with the addition of organoclay.

In comparison with NR, ENR nanocomposites exhibited shorter scorch time and cure time, and higher maximum torque, which were related to the reaction between the epoxy and amine groups. The optimum tensile strength was achieved at 8 phr of organoclay. By increasing the organoclay loading, ENR nanocomposites showed higher tensile strength but lower elongation at break compared to NR nanocomposites. This observation was attributed to the lower "strain-induced crystallisation" of the ENR matrix compared to the NR matrix. However, improvements in the mechanical properties (such as tensile strength, tensile modulus and hardness) of ENR nanocomposites were overall higher than for NR nanocomposites. This was related to the higher compatibility due to the interaction between the epoxy groups of ENR and the amine functionality of the organoclay. This contributed to the better filler-rubber interaction in organoclay-filled ENR compounds. TEM and XRD results confirmed the better dispersion of organoclay in ENR compared to NR. SEM studies showed that the enhancements in tensile strength for both NR and ENR nanocomposites were not only due to higher crosslink density, but also due to the better filler dispersion. TGA results showed that ENR nanocomposites have higher overall thermal stability with increasing organoclay loading.

5. REFERENCES

1. Pinnavaia, T. J. & Beall, G. W. **(**2000**)**. *Polymer-clay nanocomposites*. Chichester: Wiley.
2. Alexandre, M. & Dubois, P. (2000). Polymer-layered silicate nanocomposites: Preparation, properties and uses of a new class of materials. *Mater. Sci. Eng. R*, 28, 1–63.
3. Varghese, S., Tripathy, D. K., De, S. K. & Kautsch, G. K. (1990). Studies on epoxidised natural-rubber and cis-1,4-polybutadiene blend. *J. Appl. Polym.* Sci., 43, 871–875.
4. Davis, C. K. L., Gelling, I. R., Thomas, A. G. & Wolfe, S. V. (1983). Strain crystallization in random copolymers produced by epoxidation of cis 1,4-polyisoprene. *Polymer*, 24, 107–113.
5. Baker, C. S. L., Gelling I. R., Abdullah, K. A. & Smith, M. G. (1987). Compounding and applications of ENR. *Rubber World*, 196(5), 27–29.
6. Bydson, J. A. (1989). *Rubber Chemistry*. London: Springer.
7. Teh, P. L., Mohd Ishak, Z. A., Hashim, A. S., Kocsis, J. K. & Ishiaku, U. S. (2004). Effects of epoxidised natural rubber as a compatibilizer in melt compounded natural rubber-organoclay nanocomposites. *Eur. Polym. J.*, 40, 2513–2521.

8. Okada, A. & Usuki, A. (1995). The chemistry of polymer-clay hybrids. *Mater. Sci. Eng.*, C3, 109–115.
9. Novak, B. M. (1993). Hybrid nanocomposite materials–between inorganic glasses and organic polymers. *Adv. Mater.*, 5, 422–433.
10. Grannelis, E. P. (1996). Polymer layered silicate nanocomposites. *Adv. Mater*., 8, 29–35.
11. Vaia, R. A., Jandet, K. D., Kramer, E. J. & Grannelis, E. P. (1995). Synthesis of polypropylene oligomer–clay intercalation compounds. *Macromolecules*, 28, 8080–8085.
12. Mohd Ishak, Z. A., Wan, P. Y., Wong P. L., Ahmad, Z., Ishiaku, U. S., Karger-Kocsis, J. (2002). Effects of hygrothermally decomposed polyurethane on the curing and mechanical properties of carbon black-filled epoxidised natural rubber vulcanizates. *J. Appl. Polym. Sci.*, 84, 2265–2276.
13. Varghese, S., Kocsis, J. K. & Gatos, K. G. (2003). Melt compounded epoxidised natural rubber/layered silicate nanocomposites: Structure-properties relationships. *Polymer*, 44, 3977–3983.
14. Gelling, I. R. (1996). Epoxidised natural rubber. In J. C. Salomone (Ed.). *Polym. Mater. Encyc.* Florida: CRC Press. Inc., 3 (D–E), 2192–2199.
15. Ardhyanata, H., Ismail, H., Takeichi, T. & Judawisastra, H. (2006). Preparation and properties of ethylene vinyl acetate (EVA)/organoclay/ compatibilizer nanocomposites. *Polym. Plast. Technol. Eng*., 45(12), 1285–1293.
16. Ismail, H. & Munusamy, Y. (2007). Polyvinyl/Organoclay nanocomposites: Effect of filler loading and maleic anhydride. *J. Reinf. Plast. Comp.*, 26, 1681–1694.
17. Arroyo, M., Lo´pez-Manchado, M. A., Valentın, J. L. & Carretero, J. (2007). Morphology behaviour relationship of nanocomposites based on natural rubber/epoxidised natural rubber blends. *Comp. Sci. Technol*., 67, 1330–1339.
18. Mehta, S., Mirabella, F., Rufener, K. & Bafna, A. (2004). Thermoplastic olefin/clay nanocomposites: Morphology and mechanical properties. *J. Appl. Polym. Sci*., 94(2), 928–36.
19. Karger-Kocsis, J. & Zhang, Z. (2005) Structure–property relationships in nanoparticle/semicrystalline thermoplastic composites. In G. H. Michler and F. J. Baltá-Calleja (Eds.). *Mechanical properties of polymers based on nanostructure and morphology*. Florida: CRC Press, 547–596.
20. Gao, X., Mao, L., Zhang, M. & Jin, R. (2006). Polycarbonate/ polypropylene/fibrillar silicate ternary nanocomposites via two-step blending process: Degradation and morphology. *Chin. J. Chem. Eng*., 14(2), 248–252.

21. Zanetti, M., Camino, G., Thomann, R. & Mulhaupt, R. (2001). Synthesis and thermal behaviour of layered silicate–EVA nanocomposites. *Polymer*, 42(10), 4501–4507.
22. Zhang, L., Wang, Y., Wang, Y., Shui, Y. & Yu, D. (2000). Morphology and mechanical properties of clay/styrene-butadiene rubber nanocomposites. *J. Appl. Polym. Sci.*, 78, 1873–1878.